Optics Letters

Mode-selective amplification in a large mode area Yb-doped fiber using a photonic lantern

S. Wittek,* R. Bustos Ramirez, J. Alvarado Zacarias, Z. Sanjabi Eznaveh, J. Bradford, G. Lopez Galmiche, D. Zhang, W. Zhu, J. Antonio-Lopez, L. Shah, and R. Amezcua Correa

CREOL, the College of Optics and Photonics, the University of Central Florida, Orlando, Florida 32816, USA
**Corresponding author: swittek@knights.ucf.edu*

Received 18 February 2016; revised 1 April 2016; accepted 3 April 2016; posted 13 April 2016 (Doc. ID 259551); published 3 May 2016

We demonstrate selective spatial mode amplification in a few mode, double-clad Yb-doped large mode area (LMA) fiber, utilizing an all-fiber photonic lantern. Amplification to multi-watt output power is achieved while preserving high spatial mode selectivity. We observe gain values of over 12 dB for all modes: LP_{01}, LP_{11a}, and LP_{11b}, when amplified individually. Additionally, we investigate the simultaneous amplification of $LP_{01} + LP_{11a}$ and $LP_{11a} + LP_{11b}$, and the resultant mode competition. The proposed architecture allows for the reconfigurable excitation of spatial modes in the LMA fiber amplifiers, and represents a promising method that could enable dynamic spatial mode control in high power fiber lasers.

OCIS codes: (060.2320) Fiber optics amplifiers and oscillators; (060.2340) Fiber optics components.

http://dx.doi.org/10.1364/OL.41.002157

The impressive growth experienced by fiber lasers and amplifiers has been made possible due to their remarkable power scalability, excellent thermal management, and ability to be integrated into modular systems [1–3]. As such, systems with kilowatt average power or megawatt peak power are now readily available. However, due to the high optical intensity in the fiber core, both pulsed and continuous wave (CW) laser systems are limited by nonlinear effects such as four-wave mixing, self-phase modulation, stimulated Brillouin scattering, and stimulated Raman scattering [4]. In order to mitigate these undesirable nonlinear effects, extensive investigations have focused on developing advanced large mode area (LMA) fibers. However, as the mode field diameter of LMA fibers increases, it becomes more difficult to maintain effective single-mode operation and prevent the excitation of higher order modes. In the past few years, thermal mode instability (TMI) has been identified as an additional nonlinear mechanism that ultimately limits average power scaling in fiber amplifier systems [5,6]. TMI manifests itself as a sudden transition from stable single-mode operation to a regime in which the output spatial mode profile fluctuates rapidly due to power coupling between the fundamental and higher order modes [5–8]. In this regard, novel fiber amplifier architectures to overcome TMI are being investigated. For example, Otto *et al.* incorporated an acousto-optic deflector to control the spatial-modal content of the seed at the LMA fiber input to increase the threshold for TMI [9].

On the other hand, rapid progress has been made in spatial mode control and the integration of multimode fiber systems which is driven by ongoing research in spatial mode division multiplexing for optical communications [10–13]. Within this context, photonic lanterns have emerged as a powerful technology that enable modal control in multimode fiber systems [14–17]. In a mode selective photonic lantern (MSPL), several fibers of dissimilar core diameters and/or cladding diameters are stacked in a lower refractive index capillary and adiabatically tapered to form a multimode waveguide. In this case, the modes from any excited input fiber are mapped to the corresponding modes of the multimode waveguide at the lantern output [16–21].

Recently, a core pumped Er-doped few mode fiber amplifier with low mode dependent gain was demonstrated by using a six spatial MSPL [18]. Thus far, all previous demonstrations of mode selective amplification utilizing a photonic lantern have been limited to <1 W of output power [18,22].

In this work, for the first time to the best of our knowledge, we utilize an in-house fabricated MSPL for high power amplification in a Yb-doped LMA fiber. The photonic lantern provides efficient mode selective signal coupling into the Yb-doped fiber while the double-clad LMA active fiber allows amplification to the multi-watt power levels. In this work, the dynamics of the three lowest order modes (LP_{01}, LP_{11a}, and LP_{11b}) were investigated. The outlined approach provides an attractive all-fiber method to achieve spatial mode control during amplification. This appears very promising as a method to enable dynamic spatial mode control in high power fiber lasers.

The experimental setup is illustrated in Fig. 1. In order to analyze the amplifier performance, power meters, an optical spectrum analyzer (OSA), and a CCD camera were employed. A narrow-linewidth laser diode at 1064 nm was used as the seed. The 1064 nm seed wavelength was chosen, as it is spectrally distinct from amplified spontaneous emission (ASE) and self-lasing. The seed was first amplified in a 1 m long Yb-doped fiber (Nufern PM-YSF-HI), core pumped at 976 nm.

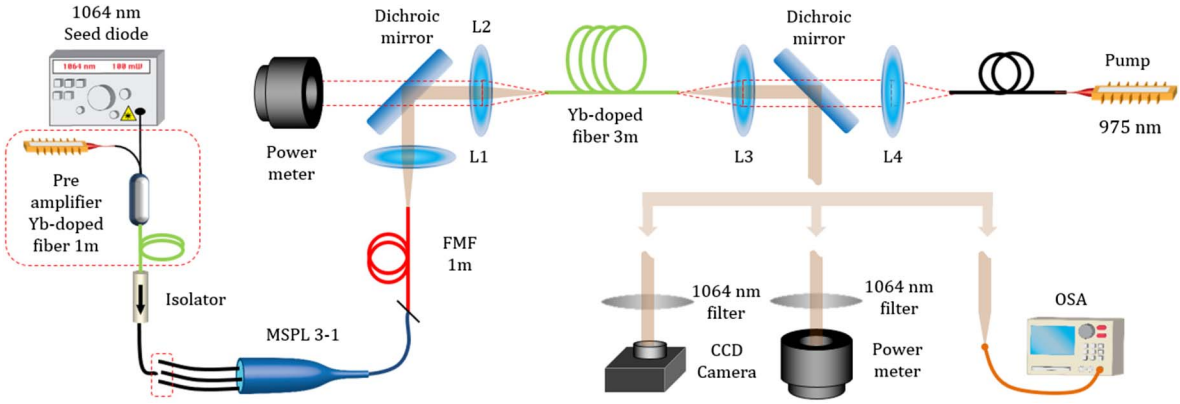

Fig. 1. Schematic of the experimental setup. A 1064 nm narrow-linewidth laser was pre-amplified and then coupled to a three mode selective photonic lantern (MSPL), which is then free-space coupled to a cladding pumped LMA Yb-doped fiber.

Pre-amplification increased the seed power to 148 mW while maintaining an optical signal to noise ratio (OSNR) of ~50 dB. The pre-amplifier output was then coupled to one of the input channels of the three mode selective lantern, which are mapped onto the LP_{01}, LP_{11a}, and LP_{11b} modes at the lantern output. Figure 2(a) depicts the photonic lantern employed in the experiment.

The near field mode profiles corresponding to the different input ports, recorded at the photonic lantern end-facet, are depicted in Fig. 2(b). Note that the slight asymmetry seen in the LP_{11b} mode can be reduced by optimizing the photonic lantern

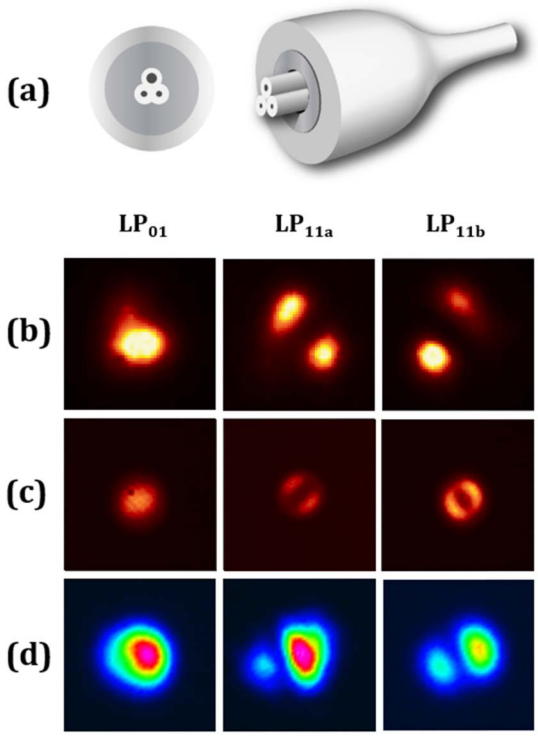

Fig. 2. (a) Illustration of the photonic lantern. (b) LP_{01}, LP_{11a}, and LP_{11b} near field mode profiles at the photonic lantern end-facet, (c) at the FMF output, and (d) amplified mode profiles through 3 m Yb-doped LMA fiber at ~5 W absorbed pump power.

fabrication process. In order to improve the coupling between the photonic lantern and the active LMA fiber, an intermediate few mode fiber (FMF) with a 15/125 μm core/cladding diameter was spliced to the photonic lantern output. The near field mode profiles after propagation through 1 m of the FMF are presented in Fig. 2(c). Figures 2(b) and 2(c) clearly demonstrate that the LP_{01}, LP_{11a}, and LP_{11b} modes can be excited by the photonic lantern with low modal cross-talk. Subsequently, the output from the FMF was free-space coupled into the 25/250 μm core/cladding diameter Yb-doped LMA fiber (Nufern PLMA-YDF-25/250-VIII) using two lenses, L1 and L2, with focal lengths of 2.86 and 4.6 mm, respectively. A dichroic mirror (HR for 1020–1080 nm, HT for 976 nm) coupled the signal into the amplifier and directed the unabsorbed pump to a power meter. The amplifier was cladding-pumped with counter-propagating light from a fiber coupled 976 nm diode with a 105/125 μm core/cladding diameter and 0.22 NA delivery fiber (nLight element E6). A dichroic mirror identical to that used at the amplifier input separated the output signal from the pump. The multimode pump was coupled to the active fiber using a pair of lenses, L3 and L4, with focal lengths of 6.24 and 8 mm, respectively. A 10 nm bandpass filter, centered at 1064 nm, was used to remove residual pump and ASE for the signal analysis as shown in Fig. 1.

In order to investigate the amplification of the LP_{01}, LP_{11a}, and LP_{11b} modes, each mode was individually excited with 77, 100, and 77 mW, respectively. The fiber amplifier was pumped with a maximum power of 25 W. Up to an absorbed pump power of ~5 W, all three modes retained good mode fidelity, as can be seen from the near field profiles presented in Fig. 2(d).

The output power versus the absorbed power for each mode is shown in Fig. 3(a). All three modes exhibited similar amplification efficiency and output signal powers. Specifically at an absorbed pump power of 4.9 W the respective modal gains were 14 dB for LP_{01}, 12 dB for LP_{11a}, and 13 dB for LP_{11b}. For an absorbed pump power of ~15 W, an output signal power of 4, 3.8, and 4.2 W was obtained for LP_{01}, LP_{11a}, and LP_{11b}, respectively.

In addition, the spectral dependence of the output signal on pump power for the LP_{11a} mode is presented in Fig. 3(b). The LP_{01} and LP_{11b} modes show a similar evolution of the spectrum with increased pump power and are not shown. At an absorbed power of 4.9 W, the OSNR was 16 dB. At this absorbed pump

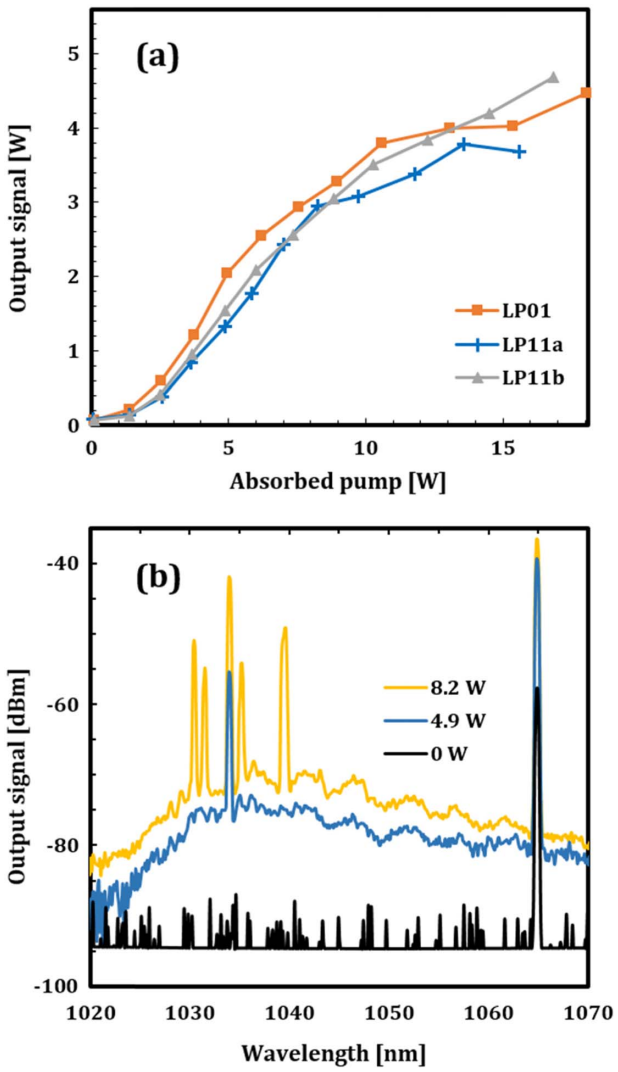

Fig. 3. (a) Measured signal output power as a function of the absorbed pump power for all three spatial modes LP_{01}, LP_{11a}, and LP_{11b} amplified individually, and (b) output spectra for the LP_{11a} mode amplification for absorbed pump power levels of 0, 4.9, and 8.2 W. The OSNRs correspond to 29, 16, and 5 dB.

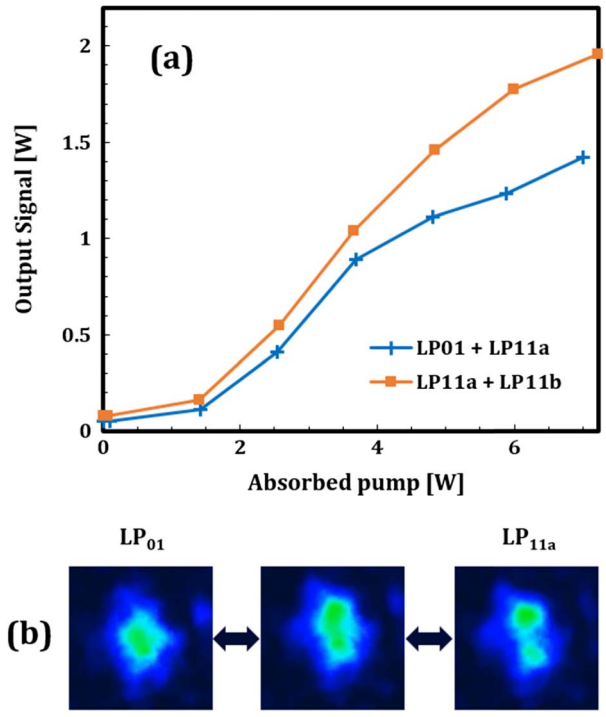

Fig. 4. (a) Simultaneous amplification of the modes LP_{01} with LP_{11a} (case 1) and LP_{11a} with LP_{11b} (case 2). (b) Three snapshots from Visualization 1 at different time steps are shown. Visualization 1 presents the near field image of the simultaneously amplified modes, LP_{01} and LP_{11a}, over 4 s. The output mode is oscillating between the LP_{01} and LP_{11a} modes due to mode competition.

power, the LP_{01} and LP_{11b} modes exhibited higher OSRNs of 24 dB. The OSNR decreased with higher pump powers as self-lasing occurred at ~1030 nm and competed with the signal amplification at 1064 nm. Characterization of OSNR between the signal and ASE/self-lasing is critical in evaluating the amplifier performance. At around 9 W of absorbed pump power, the OSNRs were 12.4, 5, and 13 dB for the LP_{01}, LP_{11a}, and LP_{11b} modes, respectively. The drastic increase of self-lasing at the absorbed pump powers above 9 W is the result of gain saturation at the seed (both spectrally and spatially). While the amplifier performance could be improved to suppress self-lasing, this is not critical for this proof of concept demonstration.

As part of additional experiments, the output of the FMF was spliced to a 50:50 fiber splitter in which the two outputs were used to excite two arms of the photonic lantern simultaneously. This enabled two cases of bi-modal amplification to be investigated: (1) amplification of LP_{01} together with LP_{11a}, and (2) amplification of LP_{11a} together with LP_{11b}. The total power of both modes launched into the Yb-doped fiber was similar for both cases (70 mW for case 1 and 98 mW for case 2). The output power measurements as a function of the absorbed pump power are shown in Fig. 4(a) for both launching conditions. The overall output efficiency is similar to the individual mode amplification, shown in Fig. 3(a).

At 5 W absorbed pump power, the total output power was 1.1 W for case 1 and 1.5 W for case 2. At this pump level, the observed OSNRs were 15.4 and 11.3 dB, respectively. For higher absorbed pump powers, the OSNRs further decreased in association with self-lasing near 1030 nm. For an absorbed pump power of 8.3 W, the OSNRs were 6 dB for case 1 and 4.1 dB for case 2.

In both cases of simultaneous amplification, mode competition was observed. As an example, three snapshots from Visualization 1 are shown in Fig. 4(b) at different time steps. Visualization 1 is a video of the amplified output modal profile in the near field for case 1 at an absorbed pump power of 100 mW. In this case, the output mode profiles oscillate from the LP_{01} to the LP_{11} mode. Visualization 1 illustrates oscillation at low Hertz-frequencies. We have separately confirmed the oscillation frequency by measuring the temporal output; however, a more detailed analysis of this is beyond the scope of this work.

In summary, we demonstrate mode selective amplification to multi-watt level average power using a three mode selective

lantern to selectively excite the LP_{01}, LP_{11a}, and LP_{11b} spatial modes in a LMA Yb-doped fiber. High spatial mode fidelity and high OSNRs were maintained for output powers of up to 2 W. With increased pump power, we observe ASE and self-lasing. Simultaneous amplification of two modes resulted in competition between the two excited modes. Research is ongoing to investigate mode competition in this amplifier configuration and to modulate the amplitude and phase of the spatial mode channels to control mode competition. Scaling to higher average power and improved modal purity can be achieved by directly splicing the photonic lantern to the active fiber. Likewise for power scaling, we are working to increase the number of spatial modes by using a photonic lantern with more input fibers [23]. Spatial mode amplification based upon photonic lantern devices coupled to LMA fiber amplifiers may open new pathways for dynamic modal control in high power fiber lasers.

Funding. Air Force Office of Scientific Research (AFOSR) (FA9550-15-10041); High Energy Lasers-Joint Technology Office (W911NF-12-1-0450); Consejo Nacional de Ciencia y Tecnología (CONACYT); Army Research Office (ARO) (W911NF-12-1-0450, W911NF-13-1-0283).

Acknowledgment. The authors thank Prysmian Group for providing the passive FMF.

REFERENCES

1. D. J. Richardson, J. Nilsson, and W. A. Clarkson, J. Opt. Soc. Am. B **27**, B63 (2010).
2. M. N. Zervas and C. A. Codemard, IEEE J. Sel. Top. Quantum Electron. **20**, 219 (2014).
3. C. Jauregui, J. Limpert, and A. Tünnermann, Nat. Photonics **7**, 861 (2013).
4. F. Stutzki, F. Jansen, T. Eidam, A. Steinmetz, C. Jauregui, J. Limpert, and A. Tünnermann, Opt. Lett. **36**, 689 (2011).
5. T. Eidam, C. Wirth, C. Jauregui, F. Stutzki, F. Jansen, H. J. Otto, O. Schmidt, T. Schreiber, J. Limpert, and A. Tünnermann, Opt. Express **19**, 13218 (2011).
6. C. Jauregui, H. J. Otto, F. Stutzki, F. Jansen, J. Limpert, and A. Tünnermann, Opt. Express **21**, 12912 (2013).
7. K. R. Hansen, T. T. Alkeskjold, J. Broeng, and J. Lægsgaard, Opt. Express **21**, 1944 (2013).
8. A. Smith and J. Smith, Opt. Express **19**, 10180 (2011).
9. H. J. Otto, C. Jauregui, F. Stutzki, F. Jansen, J. Limpert, and A. Tünnermann, Opt. Express **21**, 17285 (2013).
10. D. J. Richardson, J. M. Fini, and L. E. Nelson, Nat. Photonics **7**, 354 (2013).
11. Y. Li, W. Li, Z. Zhang, K. Miller, R. Shori, and E. G. Johnson, Opt. Express **24**, 1658 (2016).
12. Y. Yung, Q. Kang, S. Yoo, R. Sidharthan, D. Ho, P. Gregg, S. Ramachandran, S. U. Alam, and D. J. Richardson, *Optical Fiber Communication Conference Postdeadline Papers*, OSA Technical Digest (online) (Optical Society of America, 2016).
13. N. K. Fontaine, B. Huang, Z. Sanjabi Eznaveh, H. Chen, C. Jin, B. Ercan, A. Velázquez-Benetez, S. H. Chang, R. Ryf, A. Schülzgen, J. Carlos Alvarado, P. Sillard, C. Gonnet, E. Antonio-Lopez, and R. Amezcua Correa, *Optical Fiber Communication Conference Postdeadline Papers*, OSA Technical Digest (online) (Optical Society of America, 2016).
14. S. G. Leon-Saval, T. A. Birks, J. Bland-Hawthorn, and M. Englund, Opt. Lett. **30**, 2545 (2005).
15. S. G. Leon-Saval, A. Argyros, and J. Bland-Hawthorn, Opt. Express **18**, 8430 (2010).
16. T. A. Birks, I. Gris-Sanchez, S. Yerolatsitis, S. G. Leon-Saval, and R. R. Thomson, Adv. Opt. Photon. **7**, 107 (2015).
17. S. G. Leon-Saval, N. K. Fontaine, J. R. Salazar-Gil, B. Ercan, R. Ryf, and J. Bland-Hawthorn, Opt. Express **22**, 1036 (2014).
18. G. Lopez-Galmiche, Z. Sanjabi Eznaveh, L. A. Herrera Piad, A. M. Velazquez-Benitez, J. Rodriguez-Asomoza, E. Antonio-Lopez, J. J. Sanchez-Mondragon, C. Gonnet, P. Sillard, G. Li, A. Schülzgen, C. Okonkwo, and R. Amezcua-Correa, *Asia Communications and Photonics Conference*, Hong Kong (2015).
19. D. Noordegraaf, P. M. W. Skovgaard, M. D. Nielsen, and J. Bland-Hawthorn, Opt. Express **17**, 1988 (2009).
20. A. M. Velazquez-Benitez, J. Alvarado-Zacarias, G. Lopez-Galmiche, J. E. Antonio-Lopez, J. Hernandez-Cordero, J. Sanchez-Mondragon, P. Sillard, C. M. Okonkwo, and R. Amezcua-Correa, Opt. Lett. **40**, 1663 (2015).
21. S. Yerolatsitis, I. Gris-Sanchez, and T. A. Birks, Opt. Express **22**, 608 (2014).
22. J. Montoya, C. Aleshire, C. Hwang, N. K. Fontaine, A. Velázquez-Benítez, D. H. Martz, T. Y. Fan, and D. Ripin, Opt. Express **24**, 3405 (2016).
23. A. M. Velazquez-Benitez, J. E. Antonio-Lopez, J. Alvarado-Zacarias, G. Lopez-Galmiche, P. Sillard, D. Van Ras, C. Okonkwo, H. Chen, R. Ryf, N. K. Fontaine, and R. Amezcua-Correa, *European Conference on Optical Communication*, Valencia (2015).